

SOIL PHYSICAL QUALITY INDICES OF MINING-INDUCED DISTURBANCES IN SOIL WITHIN THE LOESS REGION OF WESTERN CHINA

Dejun YANG¹, Zhengfu BIAN^{1, 2}, Yajun ZHANG¹, Haochen YU², Zhenhua WU³

¹*School of Environment Science and Spatial Informatics, China University of Mining and Technology, Xuzhou, China*

²*College of Economics and Management, Qingdao University of Science and Technology, Qingdao, Shandong Province, China*

³*School of Economics and Management, China University of Mining and Technology, Xuzhou, China*

Highlights:

- the spatial variabilities of soil indices differ markedly;
- rainfall before measurements affects soil water content and particle size;
- the lower the soil water content, the higher the soil saturated hydraulic conductivity;
- the lower the soil strength, the higher the soil saturated hydraulic conductivity.

Article History:

- received 22 June 2021
- accepted 22 February 2023

Abstract. Soil sampling and in situ measurements were conducted at 24 locations at three time points from May 2015 to April 2016. The statistical analysis showed that the variabilities of soil water content and soil penetration were moderate, while particle size and soil saturated hydraulic conductivity varied considerably. Rainfall before measurements contributed positively to the mean soil water content and negatively to particle size. This was mainly due to the soil aggregates and large soil particles being broken into smaller particles from rain splash. The detached small-sized soil particles could coalesce into larger-sized ones and even soil aggregates. Stressors in zones differ, resulting in variations between soil physical quality indices. The point-to-point comparisons indicated that the mean measured soil water content and soil saturated hydraulic conductivity were similar, if the measurements for these two indices were conducted under similar weather conditions during the same period between years. The investigation on the relationships among soil physical quality indices showed a negative relationship between the measured soil water content and soil saturated hydraulic conductivity. A positive correlation was also found between soil particle size and soil saturated hydraulic conductivity. Lower soil strength resulted in higher soil saturated hydraulic conductivity.

Keywords: coal mining subsidence, particle size distribution, post-mining period, soil penetration, soil saturated hydraulic conductivity, soil water content.

Online supplementary material: Supporting information for this paper is available as online supplementary material at <https://doi.org/10.3846/jeelm.2024.19015>

 Corresponding author. E-mail: yangdj81@163.com

1. Introduction

China is the largest country in the world producing and consuming coal (Jing et al., 2018). According to the National Bureau of Statistics of China, coal output in 2018 reached 35.46 billion tons, accounting for approximately 65% of China's primary energy consumption, and more than 46% of world's coal output. It is predicted that by 2030, China's coal output will still account for approximately 50% of the total primary energy consumption, indicating that coal will remain as the main source of energy in China. About 75% of the total coal supply originates from northwestern China (Liu et al., 2015).

High-intensity exploitation of underground coal resources causes large-area surface subsidence, resulting in subsidence pits and cracks that exacerbate the destruction of the ecological environment (Jing et al., 2018; Yang et al., 2016). Land subsidence caused by underground coal mining, which accounts for 92% of the country's coal output, is one of the most prominent issues in China (Hu & Xiao, 2013). According to Bian et al. (2010), 10,000 tons of raw coal production will result in 0.2 hectares of subsided land in China. The damage includes destruction of soil structure, alteration of soil properties, limitation of vegetation growth, reduction in crop production, plant death, acceleration of soil water erosion, degradation of the landscape,

generation of cracks in the surface soil, crushing of rocks, reduction in the groundwater table, and changes in topographic and hydrologic conditions (Bian et al., 2010; Huang et al., 2015; Kuter et al., 2014; Whalley et al., 2008; Yang et al., 2016). Subsidence induced by underground coal mining will initially destroy the physical quality of the soil in the land at the time subsidence is occurring. Long term changes in the physical quality of soil will alter chemical and biological qualities, since soil physical quality greatly affects chemical and biological processes within the soil (Dexter, 2004).

Since the 1950s, there have been many studies on coal mining activities' effects on soil physical, chemical and biological indices, and the ecological environment. Bian et al. (2009) used an integrated approach involving field sampling investigation with remote sensing and ground-penetrating radar methods to observe the effects of coal mining on the soil moisture and groundwater table of the Shendong coal mining area. Pandey et al. (2014) observed the effects of air pollution and soil degradation on the community structures of woody and herbaceous plants in two different coalfields in India during 2010–2011. The effects on soil organic matter and total nitrogen distributions from coal mining subsidence in the Loess region of China were investigated previously, providing a theoretical and technical reference for land reclamation in the Loess area (Jing et al., 2018). The effect of mining subsidence on soil bacterial communities and their response to changes in the soil environment were investigated through comparisons between a controlled area and subsided area in western China (Shi et al., 2017). According to He et al. (2017), coal mining subsidence had little effect on plant diversity and community structure, and can be characterized as an intermediate disturbance to plant communities in the Daliuta coal mine of northwestern China. The impact of underground coal mining on fine root biomass, root tip count, plant available nutrient status, microbial biomass, and N mineralization rates in India has been assessed (Tripathi et al., 2009). Yang et al. (2016) investigated the effect of soil physical quality index on surface soil affected by subsidence to quantify the impact of land surface change on soil physical quality.

Other investigations paid attention to the effect of land reclamation and ecological restoration on soil indices and ecosystems during post-mining period. Krümmelbein and Raab (2012) investigated the development of bulk density, pore size distribution, and saturated hydraulic conductivity in the reclaimed land in Lusatia, Germany. The influence of herbaceous vegetation cover on the hydrological response of reclaimed mining soil was examined using simulated rainfall in the Utrillas coalfield, central-eastern Spain (Moreno-de las Heras et al., 2009). Further studies on the temporal availability and spatial distribution of soil moisture were conducted to highlight the ecological implications of vegetation in five reclaimed coal-mining slopes of Mediterranean-dry Spain subjected to different soil erosion intensities (Moreno-de las Heras et al., 2011). The infiltration rates were measured to determine the effects

of soil properties and ground cover on infiltration rates at two large reclaimed surface coal mines in Wyoming, USA (Reynolds & Lewis, 2012). Mukhopadhyay et al. (2013) developed a reclaimed mine soil index to help find tree species to reclaim coal mine degraded land. The authors found that the degraded land had significantly reduced nutrient content and soil quality as a result of the mining (Mukhopadhyay et al., 2013). Reclamation of coal mine degraded land over a short time period did not restore the overall properties of the soil, particularly the infiltration rate that has long term impact on the surrounding ecosystem (Ahirwal & Maiti, 2016). The changes in the ecosystem carbon pool and soil CO₂ flux were investigated following post-mining reclamation in dry tropical environments, and it was concluded that reclamation measures can increase the ecosystem carbon pool (Ahirwal et al., 2017). Reclamation through tree planting could improve soil quality parameters (Mukhopadhyay et al., 2016).

The Loess region in China, characterized by a loose surface, gullies, and semi-arid or arid climate, is probably the most severely eroded region in the world (Li et al., 2015a) and hence possesses a fragile ecological environment (Jing et al., 2018; Li et al., 2015a). China's coal resources are mainly distributed in the Loess Plateau region located in northwest China (Jing et al., 2018). A slight change in soil physical quality may heavily impact the vegetation restoration, plant growth, reduction of the groundwater table, and soil erosion. Studies have been conducted to maintain the balance between coal resource exploitation and environmental protection in the Loess region of western China. The authors found that soil detachment capacity was negatively correlated with sand content, cohesion, water stable aggregate, aggregate median diameter, organic matter, and root density for the red and yellow loess soils in the Loess Plateau of China (Li et al., 2015b). Factors responsible for changes in soil hydraulic conductivity of five grasslands with different vegetation restoration ages have been compared to those in a slope farmland (Ren et al., 2016).

Soil saturated hydraulic conductivity (SSHC) is a key quantitative index in arid and semi-arid areas of western China and largely determines the partitioning of precipitation into infiltration and runoff at a regional scale. The extent to which SSHC is affected by subsidence during the post-mining period is currently unknown, thereby limiting the understanding of its effect on soil water holding capacity, vegetation growth, groundwater table, and soil erosion.

The Guelph Permeameter (GP) is a popular well auger-hole instrument and is widely used for measuring SSHC on site (Reynolds & Lewis, 2012). Huang et al. (2016) used air permeability measurements combined with a limited program of GP testing to characterize spatial variability of SSHC on reclaimed soils. MacDonald et al. (2008) examined the relationships between particle size, relative density, and in situ SSHC using GP in superficial deposits in Morayshire, Northern Scotland. Further, field-scale spatial variability of SSHC by Philip-Dunne permeameter and GP was investigated on a recently constructed artificial ecosystem (Gwenzi et al., 2011).

Land-use practices such as forestry, grazing, agriculture, and mining have considerable impacts on soil hydraulic properties (Bormann & Klaassen, 2008; Gwenzi et al., 2011). Zimmermann and Elsenbeer (2008) analyzed the soil hydraulic response to regionally important disturbances and concluded that cattle grazing strongly affected the spatial mean of SSHC, but landslides did not, and that both the processes affected the spatial structure of SSHC in the topsoil. SSHC is a key soil physical quality index. Focusing on the physical qualities of disturbed soil induced by subsidence can provide guidance for land reclamation and ecological restoration during the post-mining period in the Loess region of western China.

The objectives of this study were to (1) assess the changes in soil physical indices of 24 sample sites at three time points within 12 months, (2) reveal the relationships among four soil physical indices, and (3) introduce a new SSHC prediction model during the post-mining period in the Loess region of western China.

2. Material and methods

2.1. Description of the study region

A demonstration plot located in Daliuta mining area, north of Shenmu county, Shanxi Province, northwest China, between 39.1° to 39.4° N longitudes and between 111.2° to 110.5° E latitudes, was built as a field experiment site by the China University of Mining and Technology in May 2013. This experiment site belongs to the bordering areas of Shanxi, Shaanxi, and Inner Mongolia provinces, with elevation varying from 1000 to 1500 m a.s.l (Bian et al., 2009; Yang et al., 2016). This experiment site is characterized by the transitional zone from desert to loess with a semi-arid climate, covered mainly by silt loamy loess. Dominant plants found in the study area are *Salix psammophila*, *Artemisia ordosica*, *Populus simonii*, and *Aneurotepidimu chinense* (Yang et al., 2016). Meteorological data for the study region from January 2015 to December 2016 is available in Supplemental material 1.

2.2. Description of soil sampling and in-site field experiment

The land zone above the coal mine working face (No. 52303) in the demonstration plot was previously determined from soil samples and in-situ measurements during September 2013 (before mining) and November 2013 (after mining). When the subsidence occurred during early October 2013, many ground fissures and subsided land were observed. The site slope was 0.30~0.35, with the main vegetation being *Aneurotepidimu chinense*. According to the related horizontal movement and deformation theory of mining subsidence (He et al., 2017), 24 sampling locations were distributed according to the theory of mining subsidence, which can be seen in Figure 1. ZX-1~6, YS-1~6, NLS-1~6, and WLS-1~6 were within the neutral zone, the compressive stress zone, the internal

pulling stress zone and the external pulling stress zone. There is no additional stress in the neutral zone with average reduction of surface elevation. In the compression stress zone, the soil has compressive stress, where the surface elevation changes little, and some areas are uplifted. In the external and internal pulling stress, the soil has tensile stress, where the surface elevation changes greatly, and large and deep cracks appear in some areas. Except for the group of YS-1~6, the distance between two sampling locations of the same group was about 20m. Details of the coal mine working face (No. 52303) can be seen in Yang et al. (2016). The sampling site can be seen in Figure 1. Measurements of soil physical indices were carried out at three time points during the post-mining period (May 21 to 26, 2015; October 2 to 7, 2015; and April 24 to 29, 2016). It should be noted that four heavy rainfall events (Total: 45.7 mm) occurred from September 28 to October 1, 2015.

The soil sampling depth was within 5 to 15 cm, similar to the studies of Stumpf et al. (2014) and Yang et al. (2016). The soil samples were brought back to the laboratory and measured to determine the particle size distribution (PS) using Rise-2006 Laser particle size analyzer, invented by Jinan Runzhi Technology Co., Ltd., China. Soil water content (SWC) was measured in situ with the POGO Hydra Probe Sensor. Each location was measured at three time points to calculate the mean. Soil penetration (SP) was measured via TJS-750-III Digital display instrument of soil penetration, invented by Zhejiang Top Instrument Co., Ltd., China. The measuring depth range was 0~50 cm and the maximum value was as high as 10000 kPa. In situ SSHC was measured via GP.

2.3. On-site SSHC measurement method via GP

This method involves augering a small, vertical, cylindrical well and establishing a steady discharge of water, while maintaining constant depth in the well (Bagarello, 1997). In this study, most SSHCs were determined and calculated under two heads and combined reservoir conditions. Very few measurements were made under one head and combined reservoir conditions when SSHC was comparatively higher, resulting that it only took few minutes for the water falling out of the permeameter under one water head. More than 30 determinations were made at one site to obtain a reliable estimate. Details for SSHC calculation are available in Supplemental material 2.

2.4. Statistical analysis

Descriptive statistical indices including the mean, sample variance (SV), sample standard deviation (SSD), and coefficient of variation (CV) were used. Linear regression equations were used to investigate the relationships among soil physical quality indices. Multivariable linear and log functions were used for SSHC prediction.

3. Results

3.1. Comparisons of SWC, PS, SP and SSHC in 24 measurement sites for the three time points

Figure 2 shows SWC, PS, SP and SSHC in 24 measurement sites for all three time points. All SWCs in October 2015 were higher than those in May 2015 and April 2016 (Figure 2a). The mean SWC in October 2015 (20.41%) was higher than those in both May 2015 (11.19%) and April 2016 (11.00%) (Table 1). This was mainly due to the rainfall during the last few days of September 2015 before the measurement date. The SWC range in October 2015 was higher than those in May 2015 and April 2016, while the CV of SWC in October 2015 was the lowest. The amount of rainfall in the 10, 20 and 30 days before each of the three measurements were 14.1, 20.7 and 20.9 mm for May 2015, 46.8, 52.1 and 95.9 mm for October 2015, and 0.3, 1.6 and 1.8 mm for April 2016. All SWC statistical indices during May 2015 and April 2016 had similar results, and the mean values of SWC were approximately equal.

The PS values varied among the 24 measurements performed during the same time period (Figure 2b), which could be explained by high CVs (Table 1). The CVs of PS for the three time points were 0.87, 1.25, and 0.85 respectively, advancing towards strong variability. Using the measurement in May 2015 as an example, the minimum and maximum PS were 21.64 and 342.98 μm , respectively. The mean, minimum and maximum value of PS in October 2015 and April 2016 were less than those in May 2015. For 24 sites, the statistical indices of PS in May 2015 and April 2016 were different, although the measurement periods were very similar for both 2015 and 2016.

The CVs of SP were 0.50, 0.51, and 0.42 for the three time points, with medium variability, and the values were less than those of PS. The minimum, mean, and maximum values and range of SP in October 2015 were 1623.36, 5766.01, 11111.00, and 9487.64 kPa, respectively. The minimum SP was less than 20% of the maximum. From May 2015 to April 2016, the mean SP decreased rapidly from 6614.88 kPa to 5766.01 kPa for 5 months, and continued decreasing smoothly to 5244.03 kPa for 7 months.

Figure 2d and Table 1 show that SSHCs were also variable among the 24 measurements, and this result could be explained by high CVs. CVs for the three time points were 1.19, 0.94, and 0.98, which were very close to those of PS. The minimum and maximum SSHC in May 2015 were 0.0036 and 0.46 cm/min, respectively. The maximum SSHC was 127 times higher than the minimum. Notably, the mean SSHC in April 2016 was similar to that in May 2015.

3.2. Comparison of SWC, PS, SP and SSHC in different zones

The sequence of mean SWC was NLS < WLS < ZX < YS for all three time points (Figure 2a). The PSs in four zones in October 2015 were less than those in May 2015 and April 2016 (Figure 2b). The sequence of mean PS both in

May 2015 and April 2016 was WLS < YS < NLS < ZX. The SP was the least in ZX zone and the largest in WLS zone (Figure 2c). This was mainly due to PS value wherein, lower PS caused the soil column to be denser. SSHC was the largest in ZX zone (Figure 2d). In May 2015, for example, SSHC in the ZX zone was 0.22 cm min^{-1} , four times higher than that in the NLS zone.

3.3. Point-to-point comparisons of SWC and SSHC between May 2015 and April 2016

For the point-to-point comparison of SWC between May 2015 and April 2016 (Figure 3), attempts used $y = ax$ as the fitting line of these measurements, where 24 points were distributed closely along the $y = x$ line, especially when $\text{SWC} < 12\%$. The fitting line $y = 0.9651x$, closely approached the $y = x$ line, although the correlation coefficient R^2 was only 0.292. Four points that scattered further from the $y = x$ line contributed to the relatively lower R^2 . The slope $0.9561 < 1.0$ indicated that the overall SWC measurement in April 2016 was slightly less than that in May 2015, and the result was supported by the mean SWC (Table 1).

The point-to-point comparison of SSHC between May 2015 and April 2016 obtained a relatively higher R^2 fitting line of 0.372 for SSHC (Figure 4). When SSHC was less than 0.15 cm min^{-1} , most points distributed closely along $y = x$ line. The slope, 0.8492, indicated that the overall SSHC measurement in April 2016 was less than that of May 2015. The specific point was 0.049 in May 2015 and 0.359 cm/min in April 2016 for NLS-4 zone. This may be mainly due to the complex stress and deformation in NLS-4 zone, resulting in a large SSHC gap between the two tests.

4. Discussion

4.1. Comparison of SWC, PS, SP and SSHC at 24 measurement sites at three time points

As mentioned above, mean SWC in October 2015 was the highest among the three measurement periods, where

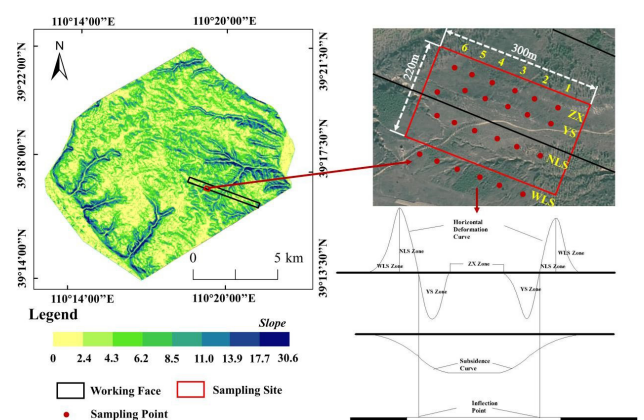


Figure 1. The locations of the study region (The slope of Daliuta; The horizontal movement and deformation theory of mining subsidence and the distribution of soil sampling locations)

mean PS in October 2015 was far less than that in the other two measurement times. This mainly resulted from rainfall during the last few days of September 2015 before the measurement date. The amount of rainfall in the 10, 20 and 30 days before October 2015 was 46.8, 52.1 and 95.9 mm. Weather conditions mostly contributed to SWC measurements, and the statistical indices of SWC were very close for the same measurement period under the similar weather conditions.

There are three interesting values in Figure 2b which are much higher than all the others. They are ZX5, YS6 and NLS5 in May 2015. One possible reason is that the soil aggregates and large-sized soil particles were not destroyed in these three sites, which could also be reflected by the high average PS (109.42 μm in May 2015). The soil aggregates and large-sized soil particles could have been detached and divided into small-sized soil particles by rain splash, resulting in 14.65 μm mean PS and 18.25 μm SSD in October 2015, which was far less than 109.42 μm and 94.72 μm in May 2015 and 60.38 μm and 51.25 μm in April 2016. This result indicated that the detached small-sized soil particles could merge into larger-sized particles, possibly forming soil aggregates again from October 2015 to April 2016 to some extent.

Since soil structure was destroyed, SP decreased approximately 1400 kPa over the course of 12 months of the post-mining period. The rate in which it decreased fluctuated, partly due to varying seasonal weather conditions.

Rainfall occurred during late spring and summer (May 2015 to October 2015), hastening the soil loosening process that destroys soil structure. From October 2015 to April 2016, low temperature and humidity froze the soil, slowing down the soil loosening process.

The mean SSHC decreased from 0.11 cm/min in May 2015 to 0.06 cm/min in October 2015. There were some possible reasons to explain this phenomenon. The soil structure was destroyed by coal mining, followed by rainfall, which caused large-sized soil particles or aggregates to break into smaller-sized particles during the post-mining period as indicated by the mean PS (Table 1). The small soil particles then made the soil column denser. Another possible reason was that the relatively higher SWC in October 2015 (20.41%) made the characteristics of the loess different from that in May 2015 (11.19%), resulting in lower SSHC.

There is one possible reason to explain why the maximum SSHC (0.46 cm/min) was 127 times higher than the minimum (0.0036 cm/min) in May 2015. This is because of the strong spatial variability (1.19) before the land subsidence. After the soil was destroyed, the CV was decreased to 0.94 in October 2015 and 0.98 in April 2016.

The mean SSHC increased from 0.06 cm/min to 0.12 cm/min from October 2015 to April 2016, indicating that the small-sized particles merged and became larger. This could also be proven by the fact that mean PS increased from 14.65 μm to 60.38 μm . The lower SWC

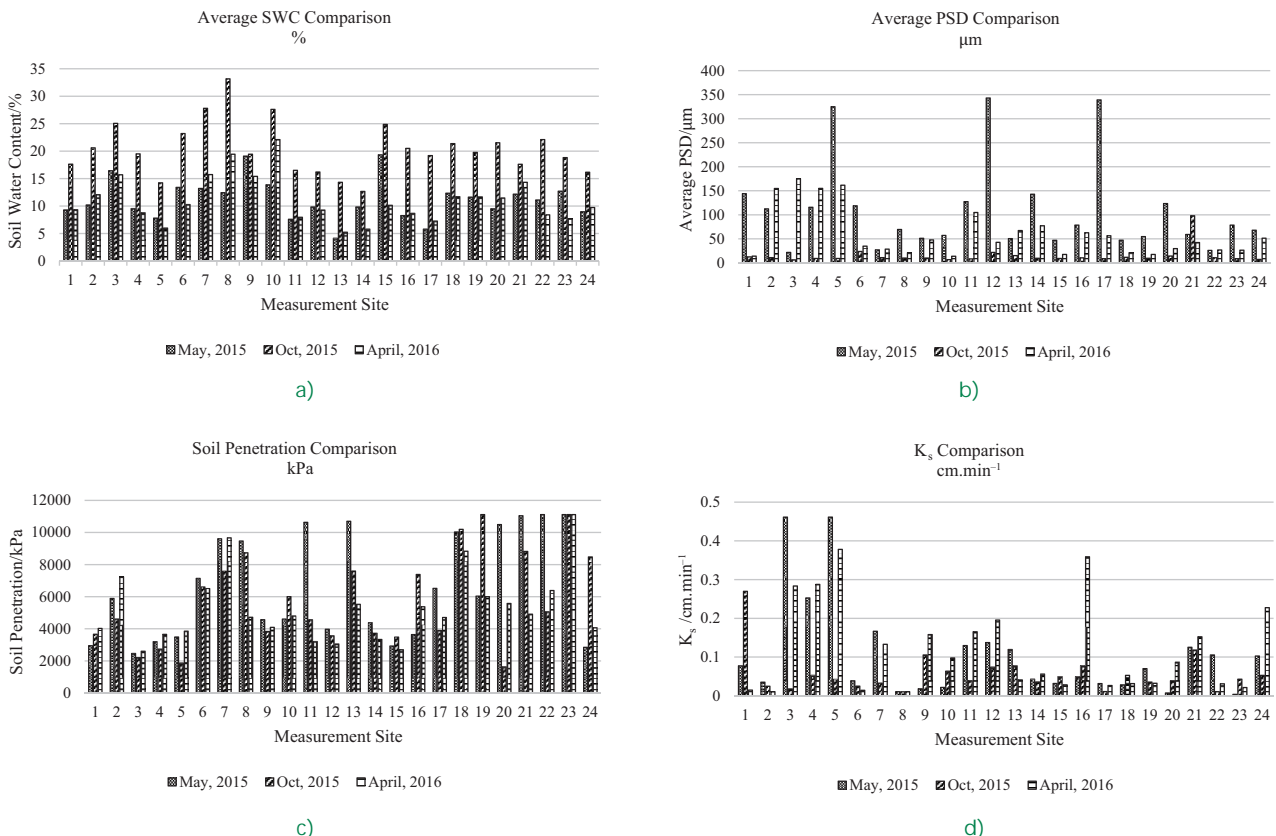


Figure 2. The SWC, PS, SP and SSHC in 24 measurement sites for all three time points (Site 1~6 is ZX1~6; Site 7~12 is YS1~6; Site 13~18 is NLS1~6; Site 19~24 is WLS1~6)

Table 1. The descriptive statistical index for the measured data in this study

	SWC			PS			SP			SSHC		
	May, 2015	Oct, 2015	April, 2016	May, 2015	Oct, 2015	April, 2016	May, 2015	Oct, 2015	April, 2016	May, 2015	Oct, 2015	April, 2016
Mean	11.19	20.41	11.00	109.42	14.65	60.38	6614.88	5766.01	5244.03	0.11	0.06	0.12
SV	13.45	23.10	18.13	8971.56	332.95	2627.01	10737488.21	8511492.73	4793015.02	1.56E-02	2.84E-03	1.34E-02
SSD	3.67	4.81	4.26	94.72	18.25	51.25	3276.81	2917.45	2189.30	0.13	0.05	0.12
CV	0.33	0.24	0.39	0.87	1.25	0.85	0.50	0.51	0.42	1.19	0.94	0.98
Min	4.13	12.67	5.23	21.64	6.23	13.67	2461.16	1623.36	2600.30	3.60E-03	1.02E-02	1.02E-02
Max	19.33	33.17	22.10	342.98	98.04	175.03	11111.00	11111.00	11111.00	0.46	0.27	0.38
Range	15.20	20.50	16.87	321.34	91.81	161.36	8649.84	9487.64	8510.71	0.46	0.26	0.37

Notes: SWC: Soil Water Content (%); PS: Particle Size (μm); SP: Soil Penetration (kPa); SSHC: Soil Saturated Hydraulic Conductivity (cm/min); SV: Sample Variance; SSD: Sample Standard Deviation; CV: Coefficient of Variation.

(11.00%) in April 2016 aided in increasing the measured SSHC to some extent, compared to the SWC (20.41%) in October 2015.

4.2. Comparison of SWC, PS, SP and SSHC in different zones

Coal mining subsidence leads to different stress characteristics, resulting in differences in soil physical quality indices. The sequence of mean SWC was NLS < WLS < ZX < YS, explained by the different levels of stress among zones. The YS zone had compressive stress, resulting in higher soil column density, while stress in both WLS and NLS zones caused the soil to loosen. The mean PS in the ZX zone both in May 2015 and April 2016 was the largest, when stress was neutral and less disturbance occurred, indicating that fewer particles were detached and carried away. SP was the least in the ZX zone and largest in the WLS zone. It was observed that PS and SP were negatively correlated with one another. SSHC was the highest in the ZX zone. Soil disturbance and the SSHC values were negatively correlated. All four indices of the different zones were affected by land subsidence, and the mechanisms of disturbance were complex and require further study. For PS, SP and SSHC, the neutral zone was quite different from the other three zones.

4.3. Point-to-point comparisons of SWC and SSHC between May 2015 and April 2016

As shown above, point-to-point comparisons of both SWC and SSHC between May 2015 and April 2016 were comparatively similar. There is one specific point (0.049 in May 2015 and 0.359 cm/min in April 2016) in NLS-4 zone in Figure 4. This may be mainly due to the complex stress and deformation in NLS-4 zone, which resulting in a large SSHC gap. Regardless of temporal variability, this was mainly due to spatial variability, although SWC and SSHC measurements were performed in the same sites. It could be concluded that if in situ measurements were done during the same period under the similar weather

conditions, measured values for these two indices would be similar.

4.4. Relationships between SSHC and SWC, PS, and SP

Although the three R^2 s (0.19, 0.37 and 0.29) in Supplemental material 3 were relatively lower, the qualitative relationship trends could still be found from the fitting lines. A negative correlation between SSHC and SWC was found in Supplemental material 3, with a 0.19 R^2 linear fitting line. The lower the measured SWC, the higher the probability of observing a higher SSHC. This could be explained by the fact that different SWC altered the characteristics of the measured loess; lower SWC causes the soil to become porous. Another possible reason was that the low SWC meant the soil column around the measured site would have similar results. The different boundary conditions among the measured sites with different measured SWC could cause the bias.

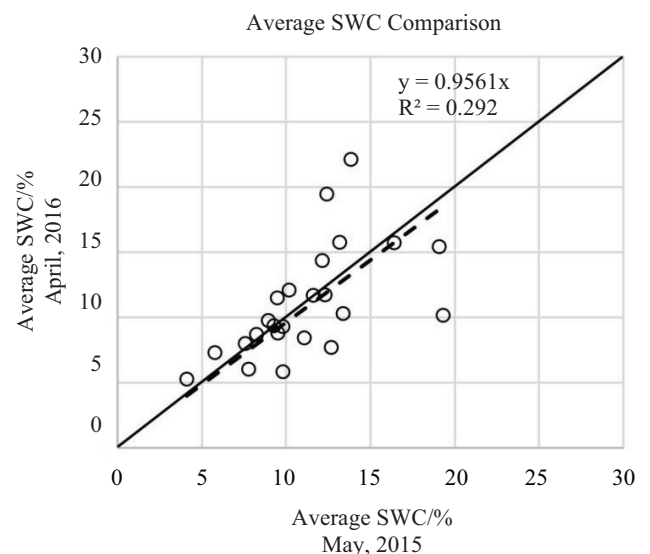


Figure 3. Point-to-point comparison of SWC between May 2015 and April 2016

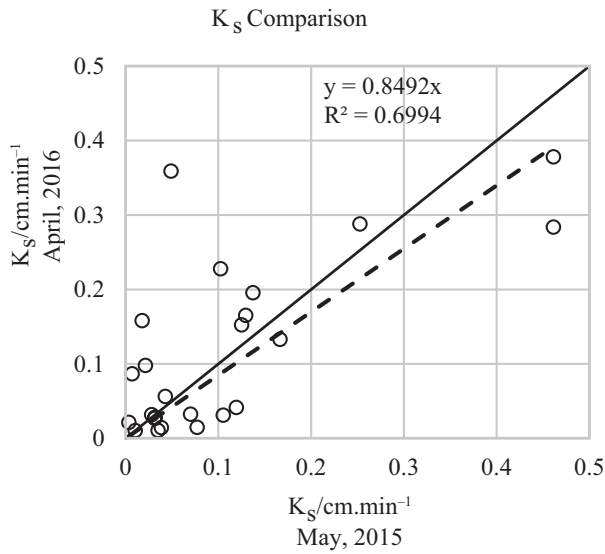


Figure 4. Point-to-point comparison of SSHC between May 2015 and April 2016

Supplemental material 3 also shows a positive correlation between SSHC and PS, and a negative correlation between SSHC and SP. The larger the PS, the larger the pore size and the larger pore sizes in the soil column provides more space for water infiltration. The lower the SP, the higher the probability of observing a higher SSHC; this is similar to how a reduction in soil strength increases the probability of obtaining a higher SSHC.

4.5. SSHC prediction by SWC, PS, and SP

Attempts were made to predict SSHC, and the two equations can be described as $SSH C = 0.00057 * PS - 0.000019 * SP - 0.0012 * SWC + 0.19$ (Linear equation) and $\text{Log}_{10}SSH C = 0.30 * \text{Log}_{10}PS - 1.14 * \text{Log}_{10}SP - 0.032 * \text{Log}_{10}SWC + 2.76$ (Log equation). Comparisons were made between measured and predicted SSHC via linear model (Supplemental material 4) and log model (Figure 5). The Log model can predict the SSHC better than linear model with a high R^2 of 0.8.

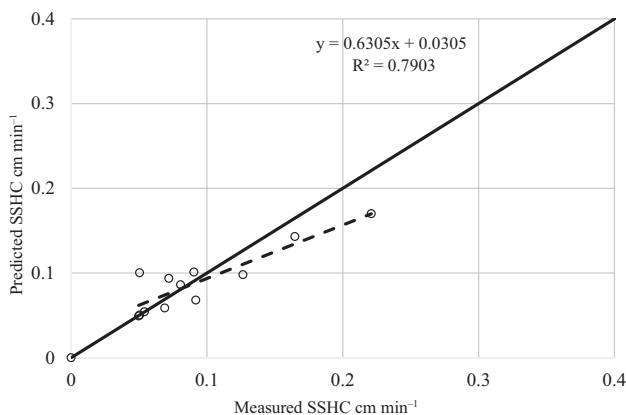


Figure 5. Comparison between measured and predicted SSHC by log model

5. Conclusions

In this paper, soil physical quality indices of soil disturbed by coal subsidence were studied using sampling and in situ measurements of 24 locations in the Loess region of western China during three time points in the post-mining period from May 2015 to April 2016.

The statistical analysis indicated that the variabilities of SWC and SP were moderate, while those of PS and SSHC were high. Rainfall before measurements mostly contributed positively to the mean values of SWC and negatively to those of PS since soil aggregates and large-sized soil particles broke apart into small-sized soil particles by rain splash. However, the detached small-sized soil particles could merge back into large-sized particles and even soil aggregates to some extent.

Different stress characteristics resulted in different soil physical quality indices. The sequence of mean SWC was $NLS < WLS < ZX < YS$ for all three measurements. The less disturbed soil in the ZX zone increased PS and decreased SP and SSHC values. Point-to-point comparisons of SWC and SSHC between May 2015 and April 2016 created fitting lines $y = 0.9651x$ and $y = 0.8492x$, respectively. This indicated that the mean measured SWC and SSHC might be similar if these two indices were measured at the same time over different years.

The relationships among soil physical quality indices were also investigated during the post-mining period. A negative relationship was found between SSHC and the measured SWC. Lower measured SWC increases the probability of observing a higher SSHC. From the relationship between SSHC and PS, the higher PS was indicative of larger pore sizes. A negative relationship was observed between SSHC and SP for all three data collections. Lower SP increases the probability of obtaining a higher SSHC. Linear and Log equations were used to predict SSHC by SWC, PS and SP. And the Log model could predict the SSHC better than linear model.

Underground mining in coal mining area will lead to caving, fracture and bending subsidence of overburden from bottom to top, resulting in a large number of cracks on the surface, which also increases the evaporation area of soil water and reduces the soil water content. Under the influence of mining, there is a certain spatial heterogeneity of soil moisture content. Soil moisture changes complex in different stress regions. Therefore, land reclamation and ecological restoration should consider taking different artificial guidance measures for different stress areas.

However, the measurements were conducted only at three time points during the 12 months of this study. For future studies, more measurements paired with soil chemical and biological quality indices measurements, should be carried out extensively over a long period of time in the Loess region of western China.

Acknowledgements

The work was supported by the Key Project of Joint Funds of the National Natural Science Foundation of China

(No. U2003103), the Special Fund for Promoting Scientific and Technological Innovation in Xuzhou in 2022 (Key Research and Development Plan (Modern Agriculture) – General project, KC22075) and the Fundamental Research Funds for the Central Universities (No. 2020ZDPYMS10).

References

- Ahirwal, J., & Maiti, S. K. (2016). Assessment of soil properties of different land uses generated due to surface coal mining activities in tropical sal (*Shorea robusta*) forest, India. *Catena*, *140*, 155–163. <https://doi.org/10.1016/j.catena.2016.01.028>
- Ahirwal, J., Maiti, S. K., & Singh, A. K. (2017). Changes in ecosystem carbon pool and soil CO₂ flux following post-mine reclamation in dry tropical environment, India. *Science of the Total Environment*, *583*, 153–162. <https://doi.org/10.1016/j.scitotenv.2017.01.043>
- Bagarello, V. (1997). Influence of well preparation on field-saturated hydraulic conductivity measured with the Guelph Permeameter. *Geoderma*, *80*, 169–180. [https://doi.org/10.1016/S0016-7061\(97\)00051-7](https://doi.org/10.1016/S0016-7061(97)00051-7)
- Bian, Z. F., Lei, S. G., Inyang, H. I., Chang, L. Q., Zhang, R. C., & Zhou, C. J., & He, X. (2009). Integrated method of RS and GPR for monitoring the changes in the soil moisture and groundwater environment due to underground coal mining. *Environmental Geology*, *57*, 131–142. <https://doi.org/10.1007/s00254-008-1289-x>
- Bian, Z., Inyang, H. I., Daniels, J. L., & Frank, O. (2010). Environmental issues from coal mining and their solutions. *International Journal of Mining Science and Technology*, *20*, 215–223. [https://doi.org/10.1016/S1674-5264\(09\)60187-3](https://doi.org/10.1016/S1674-5264(09)60187-3)
- Bormann, H., & Klaassen, K. (2008). Seasonal and land use dependent variability of soil hydraulic and soil hydrological properties of two Northern German soils. *Geoderma*, *145*, 295–302. <https://doi.org/10.1016/j.geoderma.2008.03.017>
- Dexter, A. R. (2004). Soil physical quality: Part I. Theory, effects of soil texture, density, and organic matter, and effects on root growth. *Geoderma*, *120*, 201–214. <https://doi.org/10.1016/j.geoderma.2003.09.004>
- Gwenzi, W., Hinz, C., Holmes, K., Phillips, I. R., & Mullins, I. J. (2011). Field-scale spatial variability of saturated hydraulic conductivity on a recently constructed artificial ecosystem. *Geoderma*, *166*, 43–56. <https://doi.org/10.1016/j.geoderma.2011.06.010>
- He, Y., He, X., Liu, Z., Zhao, S., Bao, L., & Li, Q., & Yan, L. (2017). Coal mine subsidence has limited impact on plant assemblages in an arid and semi-arid region of northwestern China. *Ecoscience*, *24*, 1–13. <https://doi.org/10.1080/11956860.2017.1369620>
- Huang, Y., Tian, F., Wang, Y., Wang, M., & Hu, Z. (2015). Effect of coal mining on vegetation disturbance and associated carbon loss. *Environmental Earth Sciences*, *73*, 2329–2342. <https://doi.org/10.1007/s12665-014-3584-z>
- Huang, M., Zettl, J. D., Barbour, S. L., & Pratt, D. (2016). Characterizing the spatial variability of the hydraulic conductivity of reclamation soils using air permeability. *Geoderma*, *262*, 285–293. <https://doi.org/10.1016/j.geoderma.2015.08.014>
- Hu, Z., & Xiao, W. (2013). Optimization of concurrent mining and reclamation plans for single coal seam: A case study in northern Anhui, China. *Environmental Earth Sciences*, *68*, 1247–1254. <https://doi.org/10.1007/s12665-012-1822-9>
- Jing, Z., Wang, J., Zhu, Y., & Feng, Y. (2018). Effects of land subsidence resulted from coal mining on soil nutrient distributions in a loess area of China. *Journal of Cleaner Production*, *177*, 350–361. <https://doi.org/10.1016/j.jclepro.2017.12.191>
- Krümmlbein, J., & Raab, T. (2012). Development of soil physical parameters in agricultural reclamation after brown coal mining within the first four years. *Soil & Tillage Research*, *125*, 109–115. <https://doi.org/10.1016/j.still.2012.06.013>
- Kuter, N., Dilaver, Z., & Gül, E. (2014). Determination of suitable plant species for reclamation at an abandoned coal mine area. *International Journal of Surface Mining Reclamation & Environment*, *28*, 268–276. <https://doi.org/10.1080/17480930.2014.932940>
- Liu, H., Deng, K., Lei, S., & Bian, Z. (2015). Mechanism of formation of sliding ground fissure in loess hilly areas caused by underground mining. *International Journal of Mining Science and Technology*, *25*, 553–558. <https://doi.org/10.1016/j.ijmst.2015.05.006>
- Li, Z. W., Zhang, G. H., Geng, R., & Wang, H. (2015a). Rill erodibility as influenced by soil and land use in a small watershed of the loess plateau, China. *Biosystems Engineering*, *129*, 248–257. <https://doi.org/10.1016/j.biosystemseng.2014.11.002>
- Li, Z. W., Zhang, G. H., Geng, R., Wang, H., & Zhang, X. C. (2015b). Land use impacts on soil detachment capacity by overland flow in the Loess Plateau, China. *Catena*, *124*, 9–17. <https://doi.org/10.1016/j.catena.2014.08.019>
- MacDonald, A. M., Maurice, L., Dobbs, M. R., Reeves, H. J., & Auton, C. A. (2012). Relating in situ, hydraulic conductivity, particle size and relative density of superficial deposits in a heterogeneous catchment. *Journal of Hydrology*, *434–435*, 130–141. <https://doi.org/10.1016/j.jhydrol.2012.01.018>
- Moreno-de las Heras, M., Merino-Martín, L., & Nicolau, J. M. (2009). Effect of vegetation cover on the hydrology of reclaimed mining soils under mediterranean-continental climate. *Catena*, *77*, 39–47. <https://doi.org/10.1016/j.catena.2008.12.005>
- Moreno-de las Heras, M., Espigares, T., Merino-Martín, L., & Nicolau, J. M. (2011). Water-related ecological impacts of rill erosion processes in Mediterranean-dry reclaimed slopes. *Catena*, *84*, 114–124. <https://doi.org/10.1016/j.catena.2010.10.010>
- Mukhopadhyay, S., Maiti, S. K., & Masto, R. E. (2013). Use of Reclaimed Mine Soil Index (RMSI) for screening of tree species for reclamation of coal mine degraded land. *Ecological Engineering*, *57*, 133–142. <https://doi.org/10.1016/j.ecoleng.2013.04.017>
- Mukhopadhyay, S., Masto, R. E., Yadav, A., George, J., Ram, L. C., & Shukla, S. P. (2016). Soil quality index for evaluation of reclaimed coal mine spoil. *Science of the Total Environment*, *542*(Part A), 540–550. <https://doi.org/10.1016/j.scitotenv.2015.10.035>
- Pandey, B., Agrawal, M., & Singh, S. (2014). Coal mining activities change plant community structure due to air pollution and soil degradation. *Ecotoxicology*, *23*, 1474–1483. <https://doi.org/10.1007/s10646-014-1289-4>
- Ren, Z., Zhu, L., Wang, B., & Cheng, S. (2016). Soil hydraulic conductivity as affected by vegetation restoration age on the Loess Plateau, China. *Journal of Arid Land*, *8*, 546–555. <https://doi.org/10.1007/s40333-016-0010-2>
- Reynolds, W. D., & Lewis, J. K. (2012). A drive point application of the Guelph Permeameter method for coarse-textured soils. *Geoderma*, *187–188*, 59–66. <https://doi.org/10.1016/j.geoderma.2012.04.004>
- Shi, P., Zhang, Y., Hu, Z., Ma, K., Wang, H., & Chai, T. (2017). The response of soil bacterial communities to mining subsidence in the west China aeolian sand area. *Applied Soil Ecology*, *121*, 1–10. <https://doi.org/10.1016/j.apsoil.2017.09.020>

- Stumpf, L., Pauletto, E. A., de-Castro, R. C., Spinelli-Pinto, L. F., Fontana-Fernandes, F., Stumpf da-Silva, T., Vaz-Ambus, J., Furtado-Garcia, G., Rodrigues de-Lima, C. L., & Nunes, M. R. (2014). Capability of grass in recovery of a degraded area after coal mining. *Agrociencia*, *48*, 477–487.
- Tripathi, N., Singh, R. S., & Singh, J. S. (2009). Impact of post-mining subsidence on nitrogen transformation in southern tropical dry deciduous forest, India. *Environmental Research*, *109*, 258–266. <https://doi.org/10.1016/j.envres.2008.10.009>
- Yang, D., Bian, Z., & Lei, S. (2016). Impact on soil physical qualities by the subsidence of coal mining: A case study in Western China. *Environmental Earth Sciences*, *75*, 652. <https://doi.org/10.1007/s12665-016-5439-2>
- Whalley, W. R., Watts, C. W., Gregory, A. S., Mooney, S. J., Clark, L. J., & Whitmore, A. P. (2008). The effect of soil strength on the yield of wheat. *Plant and Soil*, *306*, 237. <https://doi.org/10.1007/s11104-008-9577-5>
- Zimmermann, B., & Elsenbeer, H. (2008). Spatial and temporal variability of soil saturated hydraulic conductivity in gradients of disturbance. *Journal of Hydrology*, *361*, 78–95. <https://doi.org/10.1016/j.jhydrol.2008.07.027>